

Nuclear Transparency in a Relativistic Quark Model

Tetsu IWAMA, Akihisa KOHAMA*and Koichi YAZAKI

Department of Physics, Faculty of Science,
University of Tokyo,
7-3-1 Hongo, Bunkyo-ku, Tokyo 113, JAPAN

October 24, 2018

Abstract

We examine the nuclear transparency for the quasi-elastic ($e, e'p$) process at large momentum transfers in a relativistic quantum-mechanical model for the internal structure of the proton, using a relativistic harmonic oscillator model. A proton in a nuclear target is struck by the incident electron and then propagates through the residual nucleus suffering from soft interactions with other nucleons. We call the proton “dynamical” when we take into account of internal excitations, and “inert” when we freeze it to the ground state.

When the dynamical proton is struck with a hard (large-momentum transfer) interaction, it shrinks, *i.e.*, small-sized configuration dominates the process. It then travels through nuclear medium as a time-dependent mixture of intrinsic excited states and thus changing its size. Its absorption due to the soft interactions with nuclear medium depends on its transverse-size. Since the nuclear transparency is a measure of the absorption strength, we calculate it in our model for the dynamical case, and compare the results with those for the inert case. The effect of the internal dynamics is observed, which is in accord with the idea of the “color transparency”. We also compare our results with the experimental data in regard of q^2 -dependence as well as A -dependence, and find that the A -dependence may reveal the color-transparency effect more clearly.

Similar effects of the internal dynamics in the other semi-exclusive hard processes are briefly discussed.

*Correspondences to: kohama@tkynt2.phys.s.u-tokyo.ac.jp

1 Introduction

A phenomenon “color transparency” was predicted by Brodsky and Mueller in the early 80’s [1], [2] as a candidate of observing the effects of internal dynamics of the proton in high-energy nuclear reactions. It was speculated that the initial- and/or final-state interactions of a proton involved in a high-momentum transfer reaction with a nuclear target would be suppressed, and that the nuclear medium would look transparent ¹.

The idea of the color transparency can be explained in the following way. We call the proton “dynamical” when we take into account of internal excitations, and “inert” when we freeze it to the ground state:

- Let us consider exclusive processes, such as electron-proton or proton-proton elastic scatterings at large-momentum transfers. If we take account of the internal structure of the proton consisting of quarks and gluons, the above processes are dominated by small-sized configurations with the minimum number of constituents since the transferred large-momentum must be shared by all the constituents in the exclusive processes.
- In Quantum Chromodynamics (QCD), the interactions are mediated by the color field, but it does not couple with point-like color neutral objects, because the coupling is proportional to the color charges. Therefore, if the above exclusive processes occur in nuclear medium, the proton shortly before or after the hard process interacts weakly with the surrounding nucleons. We thus expect that the initial- and/or final-state interactions of a dynamical proton involved in such a hard semi-exclusive process with a nuclear target will be weaker than those expected for an inert proton.

The possibility of observing the color transparency in the quasi-elastic processes such as $(e, e'p)$ and $(p, 2p)$, has been discussed by many authors [6]-[14]. A novel feature of the present work is the use of a relativistic model for the internal dynamics, which will enable us to examine the prescriptions of incorporating relativistic effects in the previous discussions and tells us their importance in a transparent way.

We first introduce a quantity called “nuclear transparency”, $T(|\mathbf{k}|, \hat{\mathbf{k}}')$, for a quasi-elastic process, $(h, h'p)$, on a nuclear target, A .

$$T(|\mathbf{k}|, \hat{\mathbf{k}}') = \frac{1}{Z} \frac{1}{A(\mathbf{k})} \frac{d\sigma_{hA}}{d\Omega_{k'}} / \frac{d\sigma_{hp}}{d\Omega_{k'}}, \quad (1.1)$$

where \mathbf{k} and \mathbf{k}' are the momenta of the incident and the scattered particles, h and h' , respectively, and Z is the atomic number of the target nucleus. Here $A(\mathbf{k})$ is the Fermi-motion averaging factor. The denominator is the hp elastic differential cross section, while the quasi-elastic differential cross section in the numerator is defined by

$$\frac{d\sigma_{hA}}{d\Omega_{k'}} = \int |\mathbf{k}'|^2 d|\mathbf{k}'| d\mathbf{p} \frac{d\sigma_{hA}}{d\mathbf{k}' d\mathbf{p}}, \quad (1.2)$$

where \mathbf{p} is the recoil momentum of the struck proton.

¹For recent reviews, see Refs. [3], [4], and [5]

Our definition of the nuclear transparency is somewhat unusual in that the quasi-elastic cross section is fully integrated over the proton recoil momentum and the energy of the scattered particle. In fact, it does not correspond to what have been measured experimentally.

There have been two experimental studies of the color transparency, one with $(p, 2p)$ at BNL [15] and the other with $(e, e'p)$ at SLAC [16], [17]. In either case, the measured quantity is not exactly the transparency, $T(|\mathbf{k}|, \hat{\mathbf{k}}')$, defined here, because of the limited kinematical region covered by the experiment. We nonetheless employ this definition for our discussion, since it allows us the most reliable theoretical treatment, on the one hand, and the required measurements are accessible in future experiments, such as the Jefferson Lab. (former CEBAF), being not too far from the actually performed ones, on the other hand. The nuclear transparency defined in this way is a function of two variables, *i.e.*, the magnitude of the incident momentum, $|\mathbf{k}|$, and the scattering angle, $\theta(\mathbf{k} \wedge \mathbf{k}')$.

In the following, we deal mainly with the simpler case of electron scattering, $(e, e'p)$. In this case, since the initial- and final-state interaction of the electron can be neglected, the transparency depends only on the magnitude of the average three-momentum transfer determined by the above two variables through the free kinematics, *i.e.*,

$$T(|\mathbf{k}|, \hat{\mathbf{k}}') = T(|\bar{\mathbf{q}}|). \quad (1.3)$$

Here $|\bar{\mathbf{q}}|$ is determined by

$$|\mathbf{k}| + M = |\bar{\mathbf{k}}'| + \sqrt{\bar{\mathbf{q}}^2 + M^2}, \quad \bar{\mathbf{q}}^2 = \mathbf{k}^2 + \bar{\mathbf{k}}'^2 - 2|\mathbf{k}||\bar{\mathbf{k}}'| \cos \theta, \quad (1.4)$$

where the electron mass is ignored. M is a nucleon mass, and $\bar{\mathbf{k}}'$ is the average recoil momentum.

In $(e, e'p)$, the Fermi-motion averaging factor in eq. (1.1), $A(\mathbf{k}) \simeq 1.05$, is almost independent of \mathbf{k} [8]. A characteristic feature of the electron quasi-elastic process is that the relevant soft interaction operates only on the emitted proton whose momentum is approximately equal to the transferred momentum. The proton is thus initially struck in the longitudinal direction while the soft interaction is sensitive to its transverse size. The longitudinal-transverse correlation is therefore necessary for the color transparency to be observed in the $(e, e'p)$ process. We should keep this in our mind in constructing the model.

In this work, we use the result of the Glauber Impulse Approximation (GIA) [8] under the zero-range-no-recoil (ZRNR) approximation as a reference frame representing the case of no internal dynamics for the proton. Then we introduce a model for the internal dynamics of the proton to see the effect of the color transparency. In order to describe the internal dynamics, we use a relativistic quark model. The reason why we treat this problem in a covariant way is that, if we treat this problem non-relativistically, the internal velocity of a quark can be arbitrary large, being proportional to its momentum, and the dynamical proton could expand too fast suppressing the color transparency effect.

Two of the present authors calculated the nuclear transparency with a model emphasizing the breathing mode of the nucleon (the b -model) [14]. They included the time dilation factor to incorporate the relativistic effects as had been done in the other approaches, but there has been no justification for such a prescription. We will examine here its validity in a fully relativistic model.

We calculate the nuclear transparency for the dynamical proton in the present model, and compare it with that for the inert proton. The comparison between the two cases is expected to show us the effect of the color transparency.

The contents of this paper are organized as follows: The expression based on the Glauber approach, which does not take account of the internal dynamics and can thus be used as a reference frame for observing the “color transparency”, is reviewed in sec. 2. A formalism of incorporating the internal dynamics in calculating the nuclear transparency is briefly described in sec. 3. A relativistic harmonic oscillator model for the proton is introduced in sec. 4. We review the original version in subsec. 4.1, and introduce some modification so as to incorporate the longitudinal-transverse correlation in subsec. 4.2. The proton survival amplitude is given in subsec. 4.3. The numerical results and discussion are given in sec. 5. The importance of the relativity and the correlation in the internal dynamics will also be clarified there. The summary and the conclusion are given in sec. 6.

2 Glauber Approach

Here we quote the result of the Glauber Impulse Approximation (GIA) [8]. It is based on the Glauber multiple-scattering (not eikonal) theory [18], [19] for the proton-nucleus final-state interaction under zero-range-no-recoil (ZRNR) approximation which neglects the target nuclear recoil and the finite NN -interaction range. The nuclear transparency for $(e, e'p)$ in this approximation is given by

$$T(|\mathbf{q}|) = \int d\mathbf{r} \rho(\mathbf{r}) P^{(-)}(\mathbf{q}; \mathbf{r}), \quad (2.1)$$

where, without the nuclear correlation, the proton survival probability, $P^{(-)}(\mathbf{q}; \mathbf{r})$, can be expressed as

$$P^{(-)}(\mathbf{q}; \mathbf{r}) = \exp\{-(A-1) \sigma_{\text{NN}}^r(|\mathbf{q}|) \int_z^\infty dz' \rho(\mathbf{b}, z')\}, \quad z \parallel \mathbf{q}, \quad \mathbf{r} = (\mathbf{b}, z). \quad (2.2)$$

Here $\rho(\mathbf{r})$ is the nuclear density, and $P^{(-)}(\mathbf{q}; \mathbf{r})$ includes the effects of the final-state interactions due to multiple scattering. \mathbf{r} indicates the point where the proton has been struck, and the path of integral in eq. (2.2) is taken to be along the classical path of the struck proton. $\sigma_{\text{NN}}^r(|\mathbf{q}|)$ ($= \sigma_{\text{NN}}^{\text{total}}(|\mathbf{q}|) - \sigma_{\text{NN}}^{\text{elastic}}(|\mathbf{q}|)$) is the proton-nucleon reaction cross section at the incident momentum, $|\mathbf{q}|$.

The expressions, eqs. (2.1) and (2.2), have a simple interpretation. The proton is struck at the point \mathbf{r} and propagates along the path which is taken to be in the direction of z -axis, disappearing at the rate, $v_q \cdot \sigma_{\text{NN}}^r(|\mathbf{q}|) \cdot (A-1) \cdot \rho(\mathbf{r})$, where v_q is a proton velocity.

Introducing the time, t , by $z = v_q t$, one can regard the propagation as the time development of the struck proton in the nuclear medium. We will take such a time dependent picture in the following.

For the nuclear correlation the detailed discussions can be found in Refs. [8], [10], [11], [12].

3 Time Dependent Description

In this section, we explain the time dependent description of the internal dynamics [20], and introduce the form factor and the survival amplitude. We consider the case where the incident electron hits a proton in the target nucleus at the time, $t = 0$, and follow the time development of the struck proton as it travels in the medium.

We describe an eigenstate of a free dynamical proton as $|N; \mathbf{P}\rangle$, where N and \mathbf{P} here are a set of quantum numbers of internal excitations and the center-of-mass spatial momentum of the proton, respectively. The internal ground state corresponding to the ordinary proton is expressed by $N = 0$. The elastic form factor, $F_{\text{ep}}(q^2)$, is given by

$$F_{\text{ep}}(q^2) = \langle 0; \mathbf{P}_f | \hat{O}(q) | 0; \mathbf{P}_i \rangle, \quad (3.1)$$

where $\hat{O}(q)$ is the hard interaction operator with the four-momentum transfer, $q_\mu = P_{f,\mu} - P_{i,\mu}$. $P_{i,\mu}$ ($P_{f,\mu}$) is the four-momentum of the proton in its initial (final) state.

Then, we introduce the full hamiltonian, \hat{H} ,

$$\hat{H} = \hat{H}_0 + \hat{V}, \quad (3.2)$$

where \hat{H}_0 is the hamiltonian of the free proton with internal dynamics, and \hat{V} is the interaction between the struck proton and the surrounding nuclear medium. Thus, the time development of the dynamical proton as it travels through the nuclear medium is given by $\exp(-i\hat{H}t)$.

The desired matrix element is the probability amplitude for the system to be in the ground state of the physical proton after the interaction with the medium for a period of time, t , which is given by ²

$$M_{\text{eA}}^{(D)}(q^2; t) = \langle 0; \mathbf{P}_f | e^{-i\hat{H}t} \hat{O}(q) | 0; \mathbf{P}_i \rangle. \quad (3.3)$$

Note that $M_{\text{eA}}^{(D)}(q^2; t = 0)$ coincides with the form factor, $F_{\text{ep}}(q^2)$, eq. (3.1). For later convenience, we define a ratio, $R(q^2; t)$, by

$$R(q^2; t) \equiv M_{\text{eA}}^{(D)}(q^2; t) / (e^{-i\hat{H}_0 t} F_{\text{ep}}(q^2)). \quad (3.4)$$

The survival probability, $P^{(-)}(\mathbf{q}; \mathbf{r})$, which gives the nuclear transparency through eq. (2.1), is then given by

$$P^{(-)}(\mathbf{q}; \mathbf{r}) = |R(q^2; t(\mathbf{r}))|^2, \quad (3.5)$$

where t is the propagation time for the struck proton from the point, \mathbf{r} , to the nuclear surface. The effect of smooth nuclear surface is approximately included by taking t as

$$t(\mathbf{r}) = \frac{1}{v_{P_f} \rho_0} \int_z^\infty dz' \rho(\mathbf{b}, z'), \quad (3.6)$$

where v_{P_f} is the velocity of the struck proton, and ρ_0 is the value of $\rho(\mathbf{r})$ at the origin. The expression, eq. (3.6), is justified if the interaction strength is weak and the modification of the time evolution is proportional to the density.

²The index '(D)' represents the dynamical proton.

We also note the following property of the amplitude, $M_{\text{eA}}^{(D)}(q^2; t)$. Assuming that $\hat{V} = 0$, *i.e.*, no interaction, the matrix element becomes

$$M_{\text{eA}}^{(D)}(q^2; t) = \langle 0; \mathbf{P}_f | e^{-i\hat{H}_0 t} \hat{O}(q) | 0; \mathbf{P}_i \rangle = e^{-iE_{P_f} t} F_{\text{ep}}(q^2), \quad (3.7)$$

where we have used the fact that $|0; \mathbf{P}\rangle$ is an eigenstate of \hat{H}_0 , *i.e.*,

$$\hat{H}_0 |0; \mathbf{P}\rangle = E_P |0; \mathbf{P}\rangle, \quad (3.8)$$

where $E_P = \sqrt{M^2 + \mathbf{P}^2}$, and M denotes the proton mass.

Thus, in the absence of the interaction with the nuclear medium, $|M_{\text{eA}}^{(D)}(q^2; t)|^2$ becomes a mere squared form factor, $|F_{\text{ep}}(q^2)|^2$, and $P^{(-)}(\mathbf{q}; \mathbf{r})$ becomes unity, giving the complete transparency, $T(q) = 1$. The deviations from unity of $P^{(-)}(\mathbf{q}; \mathbf{r})$ and of $T(q)$ reflect the effects of the interaction, \hat{V} .

Next we consider the matrix element, $M_{\text{eA}}^{(I)}(q^2; t)$, for an inert proton³. The inert proton is never excited, staying only in the ground state, and $M_{\text{eA}}^{(I)}(q^2; t)$ becomes

$$M_{\text{eA}}^{(I)}(q^2; t) = e^{-i\langle \hat{H} \rangle t} F_{\text{ep}}(q^2) = e^{-i(E_{P_f} + \langle \hat{V} \rangle) t} F_{\text{ep}}(q^2). \quad (3.9)$$

Here we have defined

$$\langle \hat{O} \rangle \equiv \langle 0; \mathbf{P}_f | \hat{O} | 0; \mathbf{P}_f \rangle. \quad (3.10)$$

Following eq. (3.4), we define a similar quantity for the inert proton as

$$\begin{aligned} R_I(q^2; t) &\equiv M_{\text{eA}}^{(I)}(q^2; t) / (e^{-i\hat{H}_0 t} F_{\text{ep}}(q^2)) \\ &= e^{-i\langle \hat{V} \rangle t}. \end{aligned} \quad (3.11)$$

The survival probability, $P^{(-)}(\mathbf{q}; \mathbf{r})$, is then obtained as

$$\begin{aligned} P^{(-)}(\mathbf{q}; \mathbf{r}) &= |R_I(q^2; t(\mathbf{r}))|^2 \\ &= |\exp\{-i2\langle \hat{V} \rangle t(\mathbf{r})\}| = \exp\{2 \text{Im} \langle \hat{V} \rangle t(\mathbf{r})\}. \end{aligned} \quad (3.12)$$

The expression (3.12) becomes identical with the Glauber expression (2.2) if we take

$$-2 \text{Im} \langle 0; \mathbf{P} | \hat{V} | 0; \mathbf{P} \rangle = \frac{v_P}{\lambda} = \sigma_{\text{NN}}^r(|\mathbf{P}|) \rho_{\text{NM}} v_P. \quad (3.13)$$

Here $\sigma_{\text{NN}}^r(|\mathbf{P}|)$, ρ_{NM} and λ are the proton-nucleon reaction cross section, the nuclear matter density and the mean-free path of the proton in the nuclear matter, respectively, and we note that $\rho_{\text{NM}} \simeq (A - 1)\rho_0$ for our normalization of $\rho(\mathbf{r})$. Later we adopt the relation (3.13) in order to determine the strength of the interaction operator, \hat{V} .

³The index '(I)' represents the inert proton.

4 Formulation of the Model

In this section we briefly review the original version of the relativistic harmonic oscillator model [21], [22], [23], and then modify it for incorporating the longitudinal-transverse correlation which we introduce to describe the color transparency.

The first attempt to include the internal dynamics of the proton was made by Farrar *et al.* [6], using the model of the classically-expanding proton. Many other authors made descriptions of the internal structure of the struck proton based on the hadronic basis [7], [9], and on the non-relativistic quark model [13], [14]. Nobody has pointed out the importance of the relativity for the internal dynamics so far. This is the point that we will clarify in this work.

4.1 Relativistic Harmonic Oscillator Model

Now we introduce a relativistic quark model for the proton. A relativistic 4-dimensional harmonic oscillator model is very appropriate for our purpose, since it reproduces the elastic form factor as well as the excitation spectrum represented by the linearly rising Chew-Frautschi trajectory [21].

In this formulation the color-singlet three-quark system obeys a relativistic wave equation,

$$(P^2 - \hat{M}^2)|\Psi; \mathbf{P}\rangle = 0. \quad (4.1)$$

Here \hat{M} is the mass operator, and carries the information of the internal dynamics. An internal state of the proton is governed by an eigenvalue equation,

$$\hat{M}^2 |\phi_n; \mathbf{P}\rangle = M_n^2 |\phi_n; \mathbf{P}\rangle. \quad (4.2)$$

Here we have introduced the notation, ϕ_n , for specifying states in free space, while we use $\phi_{I,n}$ for those interacting with nuclear medium which we introduce later. The ground state, ϕ_0 , corresponds to the physical proton.

The mass operator for the three-quark system in the relativistic 4-dimensional harmonic oscillator model is given by [22]

$$-\hat{M}^2 = \eta \left(\hat{p}_r^2 + \hat{p}_s^2 + \alpha^2 (\hat{r}^2 + \hat{s}^2) \right) + C, \quad (4.3)$$

where $r^2 = r_0^2 - \mathbf{r}^2$. α is a size parameter and is chosen so as to reproduce the observed form factor. η and C are then adjusted to reproduce the proton mass of 940 [MeV] and the Roper resonance of 1440 [MeV]. These parameters are given in subsec. 5.1.

We have rearranged the coordinate four-vectors for three quarks, $\hat{x}_{1,\mu}$, $\hat{x}_{2,\mu}$, and $\hat{x}_{3,\mu}$, as follows:

$$\hat{X}_\mu = \frac{1}{3}(\hat{x}_{1,\mu} + \hat{x}_{2,\mu} + \hat{x}_{3,\mu}), \quad (4.4)$$

$$\hat{r}_\mu = \frac{1}{\sqrt{6}}(\hat{x}_{2,\mu} - \hat{x}_{3,\mu}), \quad \hat{s}_\mu = \frac{1}{3\sqrt{2}}(-2\hat{x}_{1,\mu} + \hat{x}_{2,\mu} + \hat{x}_{3,\mu}), \quad (4.5)$$

Here \hat{X}_μ is the center-of-mass coordinate, and \hat{r}_μ and \hat{s}_μ are the two independent relative coordinates which represents internal structure. The conjugate momenta are

$$\hat{P}_\mu = \hat{p}_{1,\mu} + \hat{p}_{2,\mu} + \hat{p}_{3,\mu}, \quad (4.6)$$

$$\hat{p}_{r,\mu} = \sqrt{\frac{3}{2}} (\hat{p}_{2,\mu} - \hat{p}_{3,\mu}), \quad \hat{p}_{s,\mu} = \frac{1}{\sqrt{2}} (-2\hat{p}_{1,\mu} + \hat{p}_{2,\mu} + \hat{p}_{3,\mu}). \quad (4.7)$$

The eigenvalues for time-axis are negative, and we call the highest-eigenvalue state the ‘‘ground state’’. As was discussed by Takabayashi [21], we need the additional condition;

$$\hat{P} \cdot (-i\hat{p}_r + \alpha\hat{r}) \Psi(r, s; \mathbf{P}) = \hat{P} \cdot (-i\hat{p}_s + \alpha\hat{r}) \Psi(r, s; \mathbf{P}) = 0, \quad (4.8)$$

to get the spectrum bounded from below. In the rest frame, the condition, eq. (4.8), restricts the eigenstate for time-axis to the ground state.

For a free proton at rest, *i.e.*, $\mathbf{P} = \mathbf{0}$, the ground-state wave function of the eigenvalue equation, eq. (4.2), under the condition, eq. (4.8), is

$$\phi_0(r, s; \mathbf{0}) = \left(\frac{\alpha}{\pi}\right)^2 \exp\left[-\frac{\alpha}{2} (r_0^2 + \mathbf{r}^2 + s_0^2 + \mathbf{s}^2)\right]. \quad (4.9)$$

Then, for a moving free proton which has a spatial momentum, \mathbf{P} , the eigenfunction, $\phi_0(r, s; \mathbf{P})$, should be the Lorentz-boosted form of eq. (4.9),

$$\phi_0(r, s; \mathbf{P}) = \left(\frac{\alpha}{\pi}\right)^2 \exp\left[\frac{\alpha}{2} \left\{r^2 + s^2 - \frac{2}{M_0^2} (P \cdot r)^2 - \frac{2}{M_0^2} (P \cdot r)^2\right\}\right], \quad (4.10)$$

where M_0 is the lowest eigenvalue of the mass operator, eq. (4.3). This form is manifestly covariant. Since we are interested in the case of $P_{i,\mu} = (M_0, \mathbf{0})$, and $q_\mu = (q_0, \mathbf{0}_\perp, q_3)$, eq. (4.10) becomes

$$\begin{aligned} \phi_0(r, s; \mathbf{q}) = & \left(\frac{\alpha}{\pi}\right)^2 \exp\left[\frac{\alpha}{2} \left\{r^2 + s^2 - \frac{2}{M_0^2} ((M_0 + q_0)r_0 - q_3 r_3)^2 \right. \right. \\ & \left. \left. - \frac{2}{M_0^2} ((M_0 + q_0)s_0 - q_3 s_3)^2\right\}\right]. \end{aligned} \quad (4.11)$$

Next, we consider the proton moving through the nucleus. The hamiltonian of a free proton is $\hat{H}_0 = \sqrt{\hat{M}^2 + \mathbf{q}^2}$, and the full hamiltonian of the struck proton in the medium is

$$\hat{H} = \hat{H}_0 + \hat{V} = \sqrt{\hat{M}^2 + \mathbf{q}^2} + \hat{V}. \quad (4.12)$$

We then introduce a transverse-size dependent potential due to soft interaction for the proton travelling in the nuclear medium [24]:

$$\hat{V} = -ic_0 (\hat{\mathbf{r}}_\perp^2 + \hat{\mathbf{s}}_\perp^2), \quad (4.13)$$

where \mathbf{r}_\perp and \mathbf{s}_\perp are the transverse size of the proton, and c_0 is a constant.

In the present situation, the recoil momentum of the proton is much larger than the proton mass, and thus we use the ultra-relativistic approximation for the full hamiltonian, \hat{H} , *i.e.*,

$$\hat{H} \simeq |\mathbf{q}| + \frac{\hat{M}_I^2}{2|\mathbf{q}|}, \quad (4.14)$$

where

$$-\hat{M}_I^2 = \eta \left(\hat{p}_r^2 + \hat{p}_s^2 + \alpha^2 (\hat{r}_0^2 - \hat{r}_3^2 + \hat{s}_0^2 - \hat{s}_3^2) + \alpha_\perp^2 (\hat{\mathbf{r}}_\perp^2 + \hat{\mathbf{s}}_\perp^2) \right) + C. \quad (4.15)$$

Here we have defined a ‘‘transverse’’ size parameter

$$\alpha_\perp \equiv \alpha \times \sqrt{1 - i \frac{2|\mathbf{q}|c_0}{\eta\alpha^2}}. \quad (4.16)$$

The eigenfunction, $\phi_{I,n}(r, s; \mathbf{q})$, obeys the following wave equation

$$\hat{M}_I^2 |\phi_{I,n}; \mathbf{q}\rangle = M_{I,n}^2 |\phi_{I,n}; \mathbf{q}\rangle. \quad (4.17)$$

The wave function and the mass eigenvalue are

$$\begin{aligned} \phi_{I,n}(r, s; \mathbf{q}) &= N_0^2 N'_{n_1} N'_{n_2} \cdots N_{n_6} \quad (4.18) \\ &\times \exp\left\{ \frac{\alpha}{2} (r_0^2 - r_3^2 + s_0^2 - s_3^2 - \frac{2}{M_n^2} (q' \cdot r)^2 - \frac{2}{M_n^2} (q' \cdot s)^2) \right\} \\ &\times \exp\left\{ -\frac{\alpha_\perp}{2} (\mathbf{r}_\perp^2 + \mathbf{s}_\perp^2) \right\} \\ &\times H_{n_1}(\sqrt{2\alpha_\perp} r_1) H_{n_2}(\sqrt{2\alpha_\perp} r_2) H_{n_3} \left(\sqrt{2\alpha} \sqrt{\frac{1}{M_n^2} (q' \cdot r)^2 - (r_0^2 - r_3^2)} \right) \\ &\times H_{n_4}(\sqrt{2\alpha_\perp} s_1) H_{n_5}(\sqrt{2\alpha_\perp} s_2) H_{n_6} \left(\sqrt{2\alpha} \sqrt{\frac{1}{M_n^2} (q' \cdot s)^2 - (s_0^2 - s_3^2)} \right), \end{aligned}$$

where $q'_\mu = (M + q_0, \mathbf{0}_\perp, q_3)$, $N_0^2 = \sqrt{\alpha}/\sqrt{\pi}$, $N_n^2 = \sqrt{\alpha}/(\sqrt{\pi}n!)$, $N'_n = \sqrt{\alpha_\perp}/(\sqrt{\pi}n!)$, and

$$\begin{aligned} M_{I,n}^2 &= \eta \{ -(2n_{r,0} + 1)\alpha + (2(n_1 + n_2) + 2)\alpha_\perp + (2n_3 + 1)\alpha \\ &\quad - (2n_{s,0} + 1)\alpha + (2(n_4 + n_5) + 2)\alpha_\perp + (2n_6 + 1)\alpha \} - C. \quad (4.19) \end{aligned}$$

n_i ($i = 1, \dots, 6$) are non-negative integers, and $n_{r,0} = n_{s,0} = 0$. Here also the proton is assumed to run in the z -direction. $H_n(x)$ are the Hermite polynomials defined in Appendix A.

4.2 Longitudinal-Transverse Correlation

The model in its original form has a problem in describing the color transparency. The hard scattering operator,

$$\hat{O}(q) = \exp\{iq \cdot (x_1 - X)\} = \exp\{-i\sqrt{2}q \cdot s\} \quad (4.20)$$

cannot excite the transverse modes. We have assumed that the quark, 1, has been struck. Since there is no correlation between the longitudinal motion and the transverse motion

in the original model, the transverse modes remain in their ground state, which is fatal in describing the color transparency.

The absence of the longitudinal-transverse correlation is a special feature of the harmonic oscillator model. The correlation exists in any other form of the potential. For example, Frankfurt *et al.* [25] showed that several models did contain such a correlation. We discuss the case of the Coulomb model in Appendix B, and leave more elaborate discussions to Ref. [26]. In order to remedy the defect of the model, we modify the operator, $\hat{O}(q)$, so as to incorporate the correlation in the ground state. We thus introduce a new parameter, ν , representing the strength of the correlation and replace $\hat{O}(q)$ by

$$\hat{O}(q) = \exp\{-i\sqrt{2}q \cdot s\} \times \exp\{\nu q^2(\hat{\mathbf{r}}_{\perp}^2 + \hat{\mathbf{s}}_{\perp}^2)\}, \quad (q^2 < 0). \quad (4.21)$$

We have incorporated not only the longitudinal-transverse correlation, but also the correlation among the quarks in $\hat{O}(q)$.

Then, the modified form factor, $F_{\text{ep}}^{\nu}(q^2)$, becomes,

$$\begin{aligned} F_{\text{ep}}^{\nu}(q^2) &\equiv \langle \phi_0; \mathbf{q} | e^{-i\sqrt{2}q \cdot \hat{s}} e^{\nu q^2(\hat{\mathbf{r}}_{\perp}^2 + \hat{\mathbf{s}}_{\perp}^2)} | \phi_0; \mathbf{0} \rangle \\ &= \left(1 + \nu \frac{-q^2}{\alpha}\right)^{-2} \left(1 + \frac{-q^2}{2M_0^2}\right)^{-2} \times \exp\left(-\frac{1}{2\alpha} \frac{-q^2}{1 + (-q^2)/(2M_0^2)}\right) \\ &= \left(1 + \nu \frac{-q^2}{\alpha}\right)^{-2} \times F_{\text{ep}}(q^2). \end{aligned} \quad (4.22)$$

It is well known that the original form of the form factor, *i.e.*, the case of $\nu = 0$ of eq. (4.22), gives an excellent description of the observed proton charge form factor [22]. The introduction of ν somewhat spoils the beauty and actually gives an undesirable Q^{-8} behavior at large Q^2 ($= -q^2$). However, for modest values of ν , we can choose the size parameter, α , so as to obtain a reasonable fit to the observed form factor in the relevant region of Q^2 .

4.3 Proton Survival Amplitude

We are now in the position to calculate the proton survival amplitude, $M_{\text{eA}}^{(D)}(q^2; t)$, in eq. (3.3), which can be used to obtain the proton survival probability through eq. (3.5). Inserting the complete set of the eigenstates of \hat{H} into the matrix element, we have

$$\begin{aligned} M_{\text{eA}}^{(D)}(q^2; t) &= \langle \phi_0; \mathbf{q} | e^{-i\hat{H}t} e^{-i\sqrt{2}q \cdot s} e^{\nu q^2(\hat{\mathbf{r}}_{\perp}^2 + \hat{\mathbf{s}}_{\perp}^2)} | \phi_0; \mathbf{0} \rangle \\ &= \sum_{n=0}^{\infty} \langle \phi_0; \mathbf{q} | e^{-i\hat{H}t} | \phi_{\text{I},n}; \mathbf{q} \rangle \langle \phi_{\text{I},n}; \mathbf{q} | e^{-i\sqrt{2}q \cdot s} e^{\nu q^2(\hat{\mathbf{r}}_{\perp}^2 + \hat{\mathbf{s}}_{\perp}^2)} | \phi_0; \mathbf{0} \rangle. \end{aligned} \quad (4.23)$$

The sum over n in the above expression is rather complicated due to the M_n -dependence of the wave function, $|\phi_{\text{I},n}; \mathbf{q}\rangle$. Although it could be calculated numerically since the convergence is fast, we use here an approximation of replacing M_n by M_0 in order to get a closed expression for the survival amplitude. The approximation amounts to taking the same velocity for all the intermediate states in the sum. It is justified since the M_n -dependence is not very strong and the large- n states do not contribute significantly to the sum.

Each matrix element is given as follows. The first one is

$$\begin{aligned}
\langle \phi_0; \mathbf{q} | e^{-i\hat{H}t} | \phi_{I,n}; \mathbf{q} \rangle &= e^{-i\{|\mathbf{q}| + \eta M_{I,n}^2 / (2|\mathbf{q}|)\}t} \int d^4r d^4s \phi_0(r, s; \mathbf{q}) \phi_{I,n}(r, s; \mathbf{q}) \\
&= \delta_{n_3,0} \delta_{n_6,0} \times \exp \left[-i \left\{ |\mathbf{q}| + \frac{\eta}{|\mathbf{q}|} ((n_1 + n_2 + n_4 + n_5)\alpha_\perp + 2\alpha_\perp - C/2) \right\} t \right] \\
&\quad \times \frac{4\alpha\alpha_\perp}{(\alpha_\perp + \alpha)^2} \frac{\sqrt{n_1!n_2!n_4!n_5!}}{(n_1/2)!(n_2/2)!(n_4/2)!(n_5/2)!} \left(\frac{1}{2} \frac{\alpha_\perp - \alpha}{\alpha_\perp + \alpha} \right)^{(n_1+n_2+n_4+n_5)/2}, \quad (4.24)
\end{aligned}$$

where $n_1, n_2, n_4,$ and n_5 are even. We have used eq. (A.7) in Appendix A. Another one is

$$\begin{aligned}
\langle \phi_{I,n}; \mathbf{q} | e^{-i\sqrt{2}q \cdot s} e^{\nu q^2(\hat{\mathbf{r}}_\perp^2 + \hat{\mathbf{s}}_\perp^2)} | \phi_0; \mathbf{0} \rangle &= \int d^4r d^4s \phi_{I,n}(r, s; \mathbf{q}) e^{-i\sqrt{2}q \cdot s} e^{\nu q^2(\hat{\mathbf{r}}_\perp^2 + \hat{\mathbf{s}}_\perp^2)} \phi_0(r, s; \mathbf{0}) \\
&= \delta_{n_3,0} \times \frac{4\alpha\alpha_\perp}{(\alpha + \alpha_\perp + 2\nu(-q^2))^2} \left(-i \frac{q_3}{\sqrt{\alpha}} \frac{1}{1 + (q_0/M_0)} \right)^{n_6} \\
&\quad \times \frac{\sqrt{n_1!n_2!n_4!n_5!}}{(n_1/2)!(n_2/2)!(n_4/2)!(n_5/2)!} \times \left(\frac{1}{2} \frac{\alpha_\perp - \alpha - 2\nu(-q^2)}{\alpha_\perp + \alpha + 2\nu(-q^2)} \right)^{(n_1+n_2+n_4+n_5)/2} \\
&\quad \times \left(1 + \frac{-q^2}{2M_0^2} \right)^{-2} \exp \left(-\frac{1}{2\alpha} \frac{-q^2}{1 + (-q^2)/(2M_0^2)} \right), \quad (4.25)
\end{aligned}$$

where $n_1, n_2, n_4,$ and n_5 are even. We have used eq. (A.10) in Appendix A.

Summing up the products of these matrix elements, eqs. (4.24) and (4.25), we obtain a closed form for the survival amplitude, eq. (4.23),

$$\begin{aligned}
M_{eA}^{(D)}(q^2; t) &= \sum_{n=0}^{\infty} \langle \phi_0; \mathbf{q} | e^{-i\hat{H}t} | \phi_{I,n}; \mathbf{q} \rangle \langle \phi_{I,n}; \mathbf{q} | e^{-i\sqrt{2}q \cdot s} e^{\nu q^2(\hat{\mathbf{r}}_\perp^2 + \hat{\mathbf{s}}_\perp^2)} | \phi_0; \mathbf{0} \rangle \\
&= \left(\frac{4\alpha\alpha_\perp}{(\alpha + \alpha_\perp + 2\nu(-q^2))(\alpha_\perp + \alpha)} \right)^2 \exp \left[-i \left\{ |\mathbf{q}| + \frac{\eta}{|\mathbf{q}|} (2\alpha_\perp + C/2) \right\} t \right] \\
&\quad \times \left[1 - \left(\frac{\alpha_\perp - \alpha - 2\nu(-q^2)}{\alpha_\perp + \alpha + 2\nu(-q^2)} \right) \left(\frac{\alpha_\perp - \alpha}{\alpha_\perp + \alpha} \right) \exp \left\{ -i \frac{\eta}{|\mathbf{q}|} 2\alpha_\perp t \right\} \right]^{-2} \\
&\quad \times F_{\text{ep}}(q^2). \quad (4.26)
\end{aligned}$$

Here we have used a formula,

$$\sum_{m=0}^{\infty} \frac{(2m-1)!!}{m!} (2x)^m = (1-4x)^{-1/2}. \quad (4.27)$$

The squared amplitude is given by

$$\begin{aligned}
|M_{eA}^{(D)}(q^2; t)|^2 &= |\langle \phi_0; \mathbf{q} | e^{-i\hat{H}t} e^{-i\sqrt{2}q \cdot s} e^{\nu q^2(\hat{\mathbf{r}}_\perp^2 + \hat{\mathbf{s}}_\perp^2)} | \phi_0; \mathbf{0} \rangle|^2 \\
&= \left(F_{\text{ep}}(q^2) \right)^2 \left| \frac{4\alpha\alpha_\perp}{(\alpha + \alpha_\perp + 2\nu(-q^2))(\alpha_\perp + \alpha)} \right|^4 \\
&\quad \times \left| 1 - \left(\frac{\alpha_\perp - \alpha - 2\nu(-q^2)}{\alpha_\perp + \alpha + 2\nu(-q^2)} \right) \left(\frac{\alpha_\perp - \alpha}{\alpha_\perp + \alpha} \right) \exp \left\{ -i \frac{\eta}{|\mathbf{q}|} 2\alpha_\perp t \right\} \right|^{-4} \\
&\quad \times \left| \exp \left\{ -i \frac{\eta}{|\mathbf{q}|} 2\alpha_\perp t \right\} \right|^2. \quad (4.28)
\end{aligned}$$

Finally, we obtain the ratio, $R(q^2; t)$, of eq. (3.4) as

$$\begin{aligned}
R(q^2; t) &= \left| 1 - \left(\frac{\alpha_{\perp} - \alpha - 2\nu(-q^2)}{\alpha_{\perp} + \alpha + 2\nu(-q^2)} \right) \left(\frac{\alpha_{\perp} - \alpha}{\alpha_{\perp} + \alpha} \right) \right|^4 \\
&\times \left| 1 - \left(\frac{\alpha_{\perp} - \alpha - 2\nu(-q^2)}{\alpha_{\perp} + \alpha + 2\nu(-q^2)} \right) \left(\frac{\alpha_{\perp} - \alpha}{\alpha_{\perp} + \alpha} \right) \exp\left\{-i\frac{\eta}{|\mathbf{q}|} 2\alpha_{\perp}t\right\} \right|^{-4} \\
&\times \left| \exp\left\{-i\frac{\eta}{|\mathbf{q}|} 2\alpha_{\perp}t\right\} \right|^2.
\end{aligned} \tag{4.29}$$

Given the survival probability, $P^{(-)}(\mathbf{q}; \mathbf{r}) = R(q^2; t(\mathbf{r}))$, as eq. (3.5), we can calculate the nuclear transparency using eq. (2.1).

Let us examine whether $R(q^2; t)$ and therefore $T(q)$ become unity when $Q^2 \rightarrow \infty$ in our model in accord with the idea of the color transparency. The closed expression allows us to examine the large- Q^2 behavior of the survival probability. From the definition of the transverse size parameter, α_{\perp} , the exponents of eq. (4.29) become unity, *i.e.*,

$$\exp\left\{-i\frac{\eta}{|\mathbf{q}|} 2\alpha_{\perp}t\right\} \rightarrow 1, \quad (|\mathbf{q}| \rightarrow \infty). \tag{4.30}$$

Thus, the survival probability becomes unity in the large- Q^2 limit.

ν	α [fm ⁻²]	η
0.00	11.3	0.68
0.02	15.5	0.49
0.05	21.1	0.36
0.25	53.7	0.14

Table 1: Parameters, α and η , for each fixed ν .

5 Numerical Results and Discussions

In this section we present our numerical results and discussions after we fix the parameters.

5.1 Parameters

With the modified expression for the form factor, we determine the parameter, α , so as to reproduce the observed form factor in the relevant region of Q^2 . Specifically, we require $F_{\text{ep}}^\nu(q^2) = 7.11 \times 10^{-3}$ at $Q^2 (= -q^2) = 7.512$ [(GeV/c)²] [27]. Using this value of α , we show the form factor, eq. (4.22), in Fig. 1 with the observed one. We see that the observed charge form factor of the proton is reasonably well reproduced by the modified version as long as ν is not too large.

The parameters, η and C , are adjusted to reproduce the proton mass of 940 [MeV] and the Roper resonance of 1440 [MeV]. We have assumed that the Roper resonance corresponds to a second excited state:

$$4\eta\alpha - C = M_p^2, \quad 8\eta\alpha - C = M_{\text{Roper}}^2. \quad (5.1)$$

From these relations, we obtain the value of C and a relation of $\eta\alpha$ as follows;

$$C = M_{\text{Roper}}^2 - 2M_p^2 = 7.90 \text{ [fm}^{-2}\text{]}, \quad (5.2)$$

$$\eta\alpha = \frac{1}{4}(M_{\text{Roper}}^2 - M_p^2) = 7.66 \text{ [fm}^{-2}\text{]}. \quad (5.3)$$

The numbers of α and η for each fixed ν are given in Table 1.

We then determine the parameter, c_0 , which represents the strength of the absorptive interaction, \hat{V} , using the relation, eq. (3.13), as discussed in sec. 3. We use the linearly interpolated values of the experimental proton-proton reaction cross section for $\sigma_{\text{NN}}^r(|\mathbf{q}|)$ [28], and substitute $\rho_{\text{NM}} = 0.17$ [fm⁻³] in the calculation of Figs. 2-4 and in Table 2. In calculating the nuclear transparency in Figs. 5-10, we take $\rho_{\text{NM}} \simeq (A - 1)\rho_0$, referring to the comments given in connection with eq. (3.13).

In the present model, the relation, eq. (3.13), becomes

$$\begin{aligned} -2\text{Im} \langle \hat{V} \rangle &= 2c_0 \langle \phi_0; \mathbf{q} | (\hat{\mathbf{r}}_\perp^2 + \hat{\mathbf{s}}_\perp^2) | \phi_0; \mathbf{q} \rangle \\ &= 4 \frac{c_0}{\alpha} = \sigma_{\text{NN}}^r(|\mathbf{q}|) \rho_0 v_q. \end{aligned} \quad (5.4)$$

Q^2 [(GeV/c) ²]	q_3 [GeV]	σ_{NN}^r [mb]	c_0 [fm ⁻³]			
			$\nu = 0.00$	$\nu = 0.02$	$\nu = 0.05$	$\nu = 0.25$
1	1.133	7.52	0.278	0.382	0.519	1.322
2	1.771	23.36	0.991	1.360	1.851	4.711
4	2.923	27.04	1.236	1.696	2.309	5.876
10	6.197	28.16	1.337	1.834	2.496	6.353
20	11.558	29.70	1.422	1.950	2.655	6.757
100	54.220	30.85	1.481	2.032	2.766	7.040

Table 2: Absorption strength, c_0 , for each fixed ν .

c_0 is thus determined as

$$c_0 = \frac{1}{4} \alpha \sigma_{\text{NN}}^r(|\mathbf{q}|) \rho_0 v_q. \quad (5.5)$$

The numbers of c_0 for each fixed ν are given in the Table 2.

5.2 Survival Probability

The numerical results for the ratio, $R(q^2; t)$, in eq. (4.29) with the parameters determined in the previous subsection are shown in Figs. 2-4. The difference between the curve for the inert proton and those for the dynamical proton is considered to reflect the effect of the internal dynamics. We can expect the color transparency effect to start already at Q^2 ($= -q^2$) = 4 [(GeV/c)²], and to become prominent above $Q^2 = 10$ [(GeV/c)²]. The internal dynamics gives rise to a fluctuating absorption, and effectively weakens its strength. That is, the internal dynamics could cause the color transparency, and the relativity plays an important role there.

Here we comment on the case of $\nu = 0$ as an interesting comparison. As was discussed in subsec. 4.2, the hard interaction operator, $\hat{O}(q)$, does not excite the transverse modes for $\nu = 0$. One might thus expect that this would correspond to the inert case. Actually, however, the transverse modes are excited by the interaction, \hat{V} , as the proton travels through nuclear medium, though the difference between the curves for $\nu = 0$ and the inert proton is small. The survival probability for $\nu = 0$ is that for the proton in its ground state at $t = 0$ and is a quantity relevant in discussing proton-nucleus elastic and inelastic scatterings. This is another interesting subject which can be treated in the present model, but will not be discussed further in this paper.

5.3 Nuclear Transparency

We numerically calculate the nuclear transparency for several target nuclei by the formulation in sec. 3. We parametrize the nuclear densities of ¹²C, ⁵⁶Fe, and ¹⁹⁷Au as the Woods-Saxon form,

$$\rho(\mathbf{r}) = \rho_0 \frac{1}{1 + e^{(r-c)/z}}, \quad \int d\mathbf{r} \rho(\mathbf{r}) = 1, \quad (5.6)$$

where $c = 1.1 \times A^{1/3}$ [fm] and $z = 0.53$ [fm]. The numerical results are shown in Fig. 5 as a function of q^2 , and in Figs. 6-10 as a function of the target mass number (A). The

A -dependence is included through the parameter, c , above. To include the weak q^2 -dependence of the proton-nucleon reaction cross section, we use the spline function for fitting the experimental data of the reaction cross section [28]. We see that the internal dynamics enhances the nuclear transparency as expected in Figs. 5-10.

From the results shown in Fig. 5, one would expect that the increase of the nuclear transparency due to the internal dynamics could be observed already at $Q^2 (= -q^2) = 4$ [(GeV/c)²]. This appears to contradict with the recent experiment at SLAC [16], [17], though the cases of weak longitudinal-transverse correlation have not been excluded due to its large errors. Slow increase of the transparency is still permitted.

We further calculate the target mass number dependence (A -dependence) of the nuclear transparency in the present model. The situation turns out to be more encouraging. The numerical results are shown in Figs. 6-10. In Figs. 6-8 we plot our results with the experimental data for $Q^2 = 3.06, 5.00, 6.77$ [(GeV/c)²], respectively [16] [17]. The asymptotic line of the inert proton is well fitted by $1.62 \times A^{-1/3}$. As one can see from Figs. 6 and 7, the data are almost explained by the inert proton, and the data points for heavy targets are on the line of $A^{-1/3}$, while in Fig. 8 a deviation is observed for ¹⁹⁷Au. We plot our predictions for larger Q^2 in Figs.9 and 10, and the deviations are prominent for these cases.

The importance of the A -dependence as a probe of the color transparency was previously pointed out by Ralston [29], and by Kohama, Yazaki and Seki [30]. In Ref. [30] it was found that deviations from $A^{-1/3}$ -dependence for large- A regime could be a signature of the color transparency based on a *model-independent* discussion. We call it the “off- $A^{-1/3}$ criterion”. According to the off- $A^{-1/3}$ criterion, the data point for ¹⁹⁷Au at $Q^2 = 6.77$ [(GeV/c)²] can be a signature of the color transparency, though the error is large. This data point is unique in that it deviates to the above of the asymptotic $A^{-1/3}$ line of the inert case. In Ref. [17] they fitted the data with the effective cross sections instead of the reaction cross section in the Glauber expression emphasizing the small- A data, though the $A^{-1/3}$ -dependence is universal only for large- A . Therefore we suggest that the measurement for heavy nuclei should be done with high precision, and see whether the data lie on the line of $A^{-1/3}$ or not. If the data are significantly off the line, it may signal the onset of the color transparency. The Jefferson Lab. is one of the best place to carry out this kind of experiments.

The relevant parameters in our model are η , α , and ν . For a given ν , α is determined to reproduce the charge form factor. ν is thus the crucial parameter, and it may be that we should take it smaller than 0.02 which is the smallest in our choices. If this is the case, and if the longitudinal-transverse correlation is weak, then the $(e, e'p)$ reaction may not be the best process in observing the color transparency.

In the case of $(p, 2p)$, for example, since the incident proton and the scattered proton propagate in the directions different from that of the momentum transfer, the color transparency might be more clearly observed for them, though the situation is essentially the same as that for the $(e, e'p)$ reaction for the recoil proton. The calculation of the nuclear transparency for the $(p, 2p)$ reaction is desirable, and will be done in near future.

6 Summary and Conclusions

We have constructed a relativistic quantum-mechanical model to discuss the effects of the internal structure of the proton on the nuclear transparency. The model describes the proton as a three-quark system bound by a four-dimensional harmonic oscillator potential. It reproduces both the electro-magnetic form factors of the proton and the overall features of its excitation spectrum represented by a linearly rising Chew-Frautschi trajectory very well.

We have modified the hard interaction operator, $\hat{O}(q)$, so as to incorporate the longitudinal-transverse correlation which is crucial in discussing the color transparency for $(e, e'p)$, but is absent in the original model.

The most important feature of the model is that the relativistic effects in the internal dynamics are properly taken into account and it allows us the correct treatment of the large-momentum transfer limit, *i.e.*, $Q^2 (= -q^2) \rightarrow \infty$.

The final-state interaction of the dynamical proton with the nuclear medium is taken to be purely absorptive, and the strength is assumed to be proportional to the transverse squared-size of the travelling proton. With the model specified in this way, we have calculated the proton survival probability in the nuclear medium after it is struck by the incident electron, and used the results to estimate the nuclear transparency. For comparison, we have made similar calculations for the inert proton.

The effects of the internal dynamics are clearly observed, and are found to become more and more important as the momentum transfer squared, Q^2 , increases. The nuclear transparency goes to unity as $Q^2 \rightarrow \infty$.

The present calculation is intended to discuss qualitative features of the color transparency in a specific model for the internal structure of the proton. The calculation indicates an early onset of the color transparency, which appears to contradict with the recent experiment at SLAC, though the cases of weak longitudinal-transverse correlation have not been excluded due to the large error bars of the data. The situation looks more encouraging, if we see the data from the A -dependence. We have to refine the choice of the parameters to make the model more quantitative. The strength of the longitudinal-transverse correlation is crucial in this respect, and thus the nuclear transparency of the $(e, e'p)$ offers a way of studying such details of the internal dynamics.

The hadronic process, such as $(p, 2p)$, on the other hand, may be more suitable for observing the color transparency itself, since the incident and the scattered proton can get transverse momentum transfers. The calculation of the nuclear transparency for such processes in our model will be an interesting subject for the future.

Acknowledgement

We would like to thank all the members of the nuclear theory group at University of Tokyo for their assistance and encouragement during the course of this work. A.K. and K.Y. would like to show their gratitude to Prof. N.Isgur and to Prof. F.Lenz for the discussions.

This work is supported by a Grand-Aid of the Japanese Ministry of Education, Science and Culture at the University of Tokyo (No. 08640355).

APPENDIX

A Hermite Polynomials

In this Appendix we show the definition of the Hermite polynomials, and and derive some useful formulae.

We define the Hermite polynomial in terms of the generating function as

$$e^{tx-t^2/2} = \sum_{n=0}^{\infty} \frac{t^n}{n!} H_n(x). \quad (\text{A.1})$$

Note that there are two different definitions for this functions. The factor two on the exponential is different. The orthogonality is

$$\int_{-\infty}^{\infty} dx e^{-x^2/2} H_n(x) H_m(x) = \delta_{n,m} n! \sqrt{2\pi}. \quad (\text{A.2})$$

Let us consider the one-dimensional harmonic oscillator model. The hamiltonian is given by

$$\begin{aligned} H &= -\frac{1}{2m} \frac{d^2}{dx^2} + \frac{1}{2} m \omega^2 x^2 \\ &= \frac{\omega}{2} \left(-\frac{d^2}{d\xi^2} + \xi^2 \right), \quad \xi = \alpha x, \end{aligned} \quad (\text{A.3})$$

where ξ is a dimensionless variable, and $\alpha^2 = m\omega$. The Schrödinger equation is given by

$$H \phi_n(x) = E_n \phi_n(x), \quad (\text{A.4})$$

and the wave function is

$$\phi_n(\xi) = N_n e^{-\xi^2/2} H_n(\sqrt{2}\xi), \quad N_n^2 = \frac{\alpha}{\sqrt{\pi n!}}, \quad (\text{A.5})$$

and the energy is

$$E_n = \left(n + \frac{1}{2} \right), \quad (n = 0, 1, 2, \dots). \quad (\text{A.6})$$

We then derive two formulae which are convenient to calculate matrix elements in subsec. 4.3. The first formula is

$$\int_{-\infty}^{\infty} d\xi e^{-\gamma_0 \xi^2/2} H_{2m}(\xi) = \sqrt{\frac{\pi}{\gamma_0}} \frac{(2m)!}{m!} \left(\frac{1}{4\gamma_0} - \frac{1}{2} \right)^m, \quad (m = 0, 1, 2, \dots), \quad (\text{A.7})$$

where γ_0 is complex. To prove eq. (A.7), we use the generating function, eq. (A.1), as

$$\int_{-\infty}^{\infty} d\xi \exp\left\{-\gamma_0 \xi^2 + tx - \frac{t^2}{2}\right\} = \sum_{n=0}^{\infty} \frac{t^n}{n!} \int_{-\infty}^{\infty} d\xi e^{-\gamma_0 \xi^2} H_n(\xi). \quad (\text{A.8})$$

The l.h.s. of eq. (A.8) gives

$$\begin{aligned} \int_{-\infty}^{\infty} d\eta \exp\{-\gamma_0 \eta^2 + t\xi - \frac{t^2}{2}\} &= \sqrt{\frac{\pi}{\gamma_0}} \exp\left\{\left(\frac{1}{4\gamma_0} - \frac{1}{2}\right)t^2\right\} \\ &= \sqrt{\frac{\pi}{\gamma_0}} \sum_{m=0}^{\infty} \frac{1}{m!} \left(\frac{1}{4\gamma_0} - \frac{1}{2}\right)^m t^{2m}, \end{aligned} \quad (\text{A.9})$$

where $m = 0, 1, 2, \dots$. Comparing eq. (A.9) with the r.h.s. of eq. (A.8), we obtain eq. (A.7).

The second formula is

$$\begin{aligned} &\int_{-\infty}^{\infty} d\xi e^{-s_0 \xi^2 + i\kappa \xi} H_n(\beta \xi) \\ &= \begin{cases} \sqrt{\pi/s_0} e^{-\kappa^2/(4s_0)} \left(\sqrt{1 - \frac{\beta^2}{2s_0}}\right)^n H_n\left(\frac{i\beta\kappa}{2s_0\sqrt{1 - \beta^2/(2s_0)}}\right), & (\text{if } \beta^2 \neq 2s_0) \\ \sqrt{\pi/s_0} e^{-\kappa^2/(4s_0)} (i\beta\kappa/(2s_0))^n, & (\text{if } \beta^2 = 2s_0). \end{cases} \end{aligned} \quad (\text{A.10})$$

To prove this expression, we can apply the same method as that for the first one. We then write

$$\int_{-\infty}^{\infty} d\xi \exp\{-s_0 \xi^2 + i\kappa \xi + \beta t \xi - \frac{t^2}{2}\} = \sum_{n=0}^{\infty} \frac{t^n}{n!} \int_{-\infty}^{\infty} d\xi e^{-s_0 \xi^2 + i\kappa \xi} H_n(\beta \xi). \quad (\text{A.11})$$

The l.h.s. of eq. (A.11) gives

$$\begin{aligned} &\int_{-\infty}^{\infty} d\xi \exp\{-s_0 \xi^2 + i\kappa \xi + \beta t \xi - \frac{t^2}{2}\} \\ &= \sqrt{\frac{\pi}{s_0}} \exp\left(-\frac{\kappa^2}{4s_0}\right) \times \exp\left\{-\frac{1}{2}\left(1 - \frac{\beta^2}{2s_0}\right)t^2 + \frac{1}{2s_0}i\beta t \kappa\right\} \\ &= \sqrt{\frac{\pi}{s_0}} \exp\left(-\frac{\kappa^2}{4s_0}\right) \times \sum_{n=0}^{\infty} \frac{t^n}{n!} \left(\sqrt{1 - \frac{\beta^2}{2s_0}}\right)^n H_n\left(\frac{i\beta\kappa}{2s_0\sqrt{1 - (\beta^2/2s_0)}}\right). \end{aligned} \quad (\text{A.12})$$

If $\beta^2 = 2s_0$, then the l.h.s. of eq. (A.11) gives

$$\begin{aligned} \int_{-\infty}^{\infty} d\xi \exp\{-s_0 \xi^2 + i\kappa \xi + \beta t \xi - \frac{t^2}{2}\} &= \sqrt{\frac{\pi}{s_0}} \exp\left(-\frac{\kappa^2}{4s_0}\right) \exp\left\{\frac{i\beta\kappa}{2s_0}t\right\} \\ &= \sqrt{\frac{\pi}{s_0}} \exp\left(-\frac{\kappa^2}{4s_0}\right) \sum_{n=0}^{\infty} \frac{t^n}{n!} \left(\frac{i\beta\kappa}{2s_0}\right)^n \end{aligned} \quad (\text{A.13})$$

If we compare eqs. (A.12) and (A.13) with the r.h.s. of eq. (A.11), we obtain eq. (A.10).

B Case of the Coulomb Potential

In subsec. 4.2, we have modified the hard interaction operator, $\hat{O}(q)$, so as to incorporate the longitudinal-transverse correlation which is crucial in discussing the color transparency, but is absent in the harmonic oscillator model. The correlation strength is represented by the parameter, ν , but we have no *a priori* basis for determining the strength. Here, we use a non-relativistic Coulomb model to get a rough idea of the strength.

In the Coulomb model, the ground state is given by

$$\phi_{c,0}(r) = 2\alpha_c^{3/2} e^{-\alpha_c r}. \quad (\text{B.1})$$

Here, α_c is determined as

$$\begin{aligned} \langle \mathbf{r}^2 \rangle &\equiv \langle \phi_{c,0} | \mathbf{r}^2 | \phi_{c,0} \rangle = 3/\alpha_c^2 = (0.853)^2 \text{ [fm}^2\text{]}, \\ &\Leftrightarrow \alpha_c^2 = \frac{3}{\langle \mathbf{r}^2 \rangle}. \end{aligned} \quad (\text{B.2})$$

We use $\langle \mathbf{r}^2 \rangle = (0.853)^2 \text{ [fm}^2\text{]}$.

We introduce the following quantity to see the correlation strength. It becomes unity in the absence of correlation.

$$\left(\frac{2}{3} \langle \mathbf{r}^2 \rangle \right)^{-1} \times \frac{\langle \phi_{c,0} | (x^2 + y^2) e^{iqz} | \phi_{c,0} \rangle}{\langle \phi_{c,0} | e^{iqz} | \phi_{c,0} \rangle} = \left(1 + \frac{|\mathbf{q}|^2}{4\alpha_c^2} \right)^{-1}, \quad (\text{B.3})$$

where the first term is introduced for the normalization. We can see that the correlation effect is appreciable at a large-momentum transfers.

We now calculate the same quantity in a non-relativistic harmonic oscillator model with ν being introduced in a way analogous to the relativistic model:

$$\left(\frac{2}{3} \langle \mathbf{r}^2 \rangle \right)^{-1} \times \frac{\langle \phi_{h.o.,0} | (x^2 + y^2) e^{-\nu q^2(x^2+y^2)} e^{iqz} | \phi_{h.o.,0} \rangle}{\langle \phi_{h.o.,0} | e^{-\nu q^2(x^2+y^2)} e^{iqz} | \phi_{h.o.,0} \rangle} = \left(1 + \frac{\nu |\mathbf{q}|^2}{\alpha_{h.o.}} \right)^{-1}. \quad (\text{B.4})$$

α_0 is determined as

$$\begin{aligned} \langle \mathbf{r}^2 \rangle &\equiv \langle \phi_{h.o.,0} | \mathbf{r}^2 | \phi_{h.o.,0} \rangle = 3/\alpha_{h.o.}, \\ &\Leftrightarrow \alpha_{h.o.} = \frac{3}{\langle \mathbf{r}^2 \rangle}. \end{aligned} \quad (\text{B.5})$$

Thus, $\nu = 1/4$ for the Coulomb model. It seems that among the commonly-used binding potentials, the Coulomb potential has the strongest correlation. We take this value for ν as the maximum in our calculation for the nuclear transparency.

References

- [1] S.J.Brodsky, *Proceedings of the 13th International Symposium on Multiparticle Dynamics 1982*, ed. W.Kittel, W.Metzger, and A.Stergiou, *World Scientific* (1982) 963; A.H.Mueller, *Proceedings of the 17th Rencontre de Moriond (Les Arcs, 1982)*, ed. J.Tran Thanh Van, (*Editions Frontiers, Paris*), (1982).
- [2] S.J.Brodsky and A.H.Mueller, *Phys. Lett.*, **B206** (1988) 685.
- [3] N.N.Nikolaev, *Lecture note for RCNP Kikuchi School on Spin Physics at Intermediate Energies*, (1992) “High Energy Nuclear Reaction in QCD: Colour Transparency Aspects”.
- [4] L.L.Frankfurt, G.A.Miller, M.Strikman, *Annu. Rev. Nucl. Part. Sci.*, **45** (1994) 501.
- [5] P.Jain, B.Pire, and J.P.Ralston, *Phys. Rep.*, **271** (1996) 67.
- [6] G.R.Farrar, H.Liu, L.L.Frankfurt and M.I.Strikman, *Phys. Rev. Lett.*, **61** (1988) 686.
- [7] B.K.Jennings and G.A.Miller, *Phys. Lett.*, **B236** (1990) 209.
- [8] A.Kohama, K.Yazaki, and R.Seki, *Nucl. Phys.*, **A536** (1992) 716; *Nucl. Phys.*, **A551** (1993) 687.
- [9] N.N.Nikolaev, A.Szczurek, J.Speth, J.Wambach, B.G.Zhakharov, V.R.Zoller, *Nucl. Phys.*, **A567** (1994) 781.
- [10] N.N.Nikolaev, A.Szczurek, J.Speth, J.Wambach, B.G.Zhakharov, and V.R.Zoller, *Phys. Lett.*, **B317** (1993) 281.
- [11] R.Seki, T.D.Shoppa, A.Kohama, and K.Yazaki, *Phys. Lett.*, **B383** (1996) 133.
- [12] A.S.Rinat and M.F.Taragin, *Nucl. Phys.*, **A597** (1996) 636.
- [13] B.Z.Kopeliovich and B.G.Zakharov, *Phys. Lett.*, **B264** (1991) 434.
- [14] A.Kohama and K.Yazaki, *Nucl. Phys.*, **A575** (1994) 645; K.Yazaki and A.Kohama, *Hadrons and Nuclei from QCD*, ed. K.Fujii, Y.Akaishi, and B.L.Reznik, *World Scientific, Singapore*, (1994) 10.
- [15] A.S.Carroll *et al.*, *Phys. Rev. Lett.*, **61** (1988) 1698.
- [16] N.C.R.Makins *et al.*, *Phys. Rev. Lett.*, **72** (1994) 1986.
- [17] T.G.O’Neill, *et al.*, *Phys. Lett.*, **B351** (1995) 87.
- [18] A.K.Kerman, H.McManus and R.M.Thaler, *Ann. Phys.*, **8** (1959) 551.
- [19] R.J.Glauber, *Lectures in Theoretical Physics*, ed. W.E.Brittin and D.G.Dunham, *Interscience, New York*, **Vol.1** (1959) 315.

- [20] K.Yazaki, T.Iwama, and A.Kohama,
Recent Developments in Particle and Nuclear Theory,
ed. W.Bentz, G.T.Park, and H.S.Song,
Jour. of the Korean Phys. Soc., Suppl., **29** (1996) S388.
- [21] T.Takabayashi, *Phys. Rev.*, **139** (1965) B1381;
Suppl. Prog. Theo. Phys., **Extra Number** (1965) 339.
- [22] K.Fujimura, T.Kobayashi and M.Namiki, *Prog. Theor. Phys.*, **43** (1970) 73;
Prog. Theor. Phys., **44** (1970) 193.
- [23] R.P.Feynman, M.Kislinger, and F.Ravndal, *Phys. Rev.*, **D3** (1971) 2706.
- [24] F.E.Low, *Phys. Rev.*, **D12** (1975) 163;
S.Nussinov, *Phys. Rev. Lett.*, **34** (1975) 1286; *Phys. Rev.*, **D14** (1976) 246;
G.Bertsch, S.J.Brodsky, A.S.Goldhaber and J.G.Gunion,
Phys. Rev. Lett., **47** (1981) 297;
A.B.Zamolodchikov, B.Z.Kopeliovich, and L.I.Lapidus, *JETP Lett.*, **33** (1981) 595;
J.F.Gunion and D.E.Soper, *Phys. Rev.*, **D15** (1977) 2617.
- [25] L.Frankfurt, G.A.Miller and M.Strikman, *Nucl. Phys.*, **A555** (1993) 752.
- [26] D.Makovoz and G.A.Miller, *Phys. Rev.*, **C51** (1995) 2716.
- [27] D.H.Coward, *et al.*, *Phys. Rev. Lett.*, **20** (1968) 292;
P.N.Kirk, *et al.*, *Phys. Rev.*, **D8** (1973) 63.
- [28] J.Bystricky *et al.*, *LANDOLT-BÖRNSTEIN. New Series.*, I/9a (1980) 17.
- [29] J.P.Ralston, in *Perspectives in Hadron Structure*, ed. M.Harakeh, *et al.*,
(NATO Adv. Study Inst., Dronon, the Netherlands, 1993).
- [30] A.Kohama, K.Yazaki, and R.Seki, *Phys. Lett.*, **B344** (1995) 61;
Prog. Theo. Phys. Suppl., **120** (1995) 277.

Figure Captions

Figure 1

A comparison of the electromagnetic form factors, $F_{\text{ep}}^\nu(q^2)$, of the proton in the present model with experimental data. The dotted curve is the form factor of the original harmonic oscillator model ($\nu = 0$). The solid curve, the dashed curve, and the dot-dashed curve are those of the modified harmonic oscillator model with $\nu = 0.02, 0.05, 0.25$, respectively. The crosses and the circles indicate the experimental data from Ref. [27].

Figure 2

The time development of the ratio, $|R(q^2; t)|^2$, eq. (4.29), for $Q^2 (= -q^2) = 10$ $[(\text{GeV}/c)^2]$. The dotted curve is the case of the inert proton. The solid curve, the dashed curve, and the dot-dashed curve are those of the dynamical proton with $\nu = 0.02, 0.05, 0.25$, respectively.

Figure 3

The time development of the ratio, $|R(q^2; t)|^2$, eq. (4.29), for $Q^2 (= -q^2) = 20$ $[(\text{GeV}/c)^2]$. The curves are the same as those of Fig. 3.

Figure 4

The time development of the ratio, $|R(q^2; t)|^2$, eq. (4.29), for $Q^2 (= -q^2) = 100$ $[(\text{GeV}/c)^2]$. The curves are the same as those of Fig. 3.

Figure 5

A comparison of the nuclear transparency with experimental data for ^{12}C , ^{56}Fe , and ^{197}Au as a function of $Q^2 (= -q^2)$. The dotted curve is the case of the inert proton. The solid, dashed, and dot-dashed curves are the case of the dynamical proton with $\nu = 0.02, 0.05, 0.25$, respectively. The data are from Ref. [17].

Figure 6

A comparison of the nuclear transparency with experimental data for ^{12}C , ^{56}Fe , and ^{197}Au as a function of the target mass number, A . $Q^2 (= -q^2) = 3.06$ $[(\text{GeV}/c)^2]$. The dotted curve is the case of the inert proton. The solid, dashed, and dot-dashed curves are the case of the dynamical proton with $\nu = 0.02, 0.05, 0.25$, respectively. The data are from Ref. [17].

Figure 7

A comparison of the nuclear transparency with experimental data for ^{12}C , ^{56}Fe , and ^{197}Au as a function of the target mass number, A . $Q^2 (= -q^2) = 5.00$ $[(\text{GeV}/c)^2]$. The curves are the same as those of Fig. 6.

Figure 8

A comparison of the nuclear transparency with experimental data for ^{12}C , ^{56}Fe , and ^{197}Au as a function of the target mass number, A . $Q^2 (= -q^2) = 6.77$ $[(\text{GeV}/c)^2]$. The curves

are the same as those of Fig. 6.

Figure 9

The nuclear transparency as a function of the target mass number, A . $Q^2 (= -q^2) = 10.0$ [(GeV/c)²]. The curves are the same as those of Fig. 6.

Figure 10

The nuclear transparency as a function of the target mass number, A . $Q^2 (= -q^2) = 20.0$ [(GeV/c)²]. The curves are the same as those of Fig. 6.

Fig.1

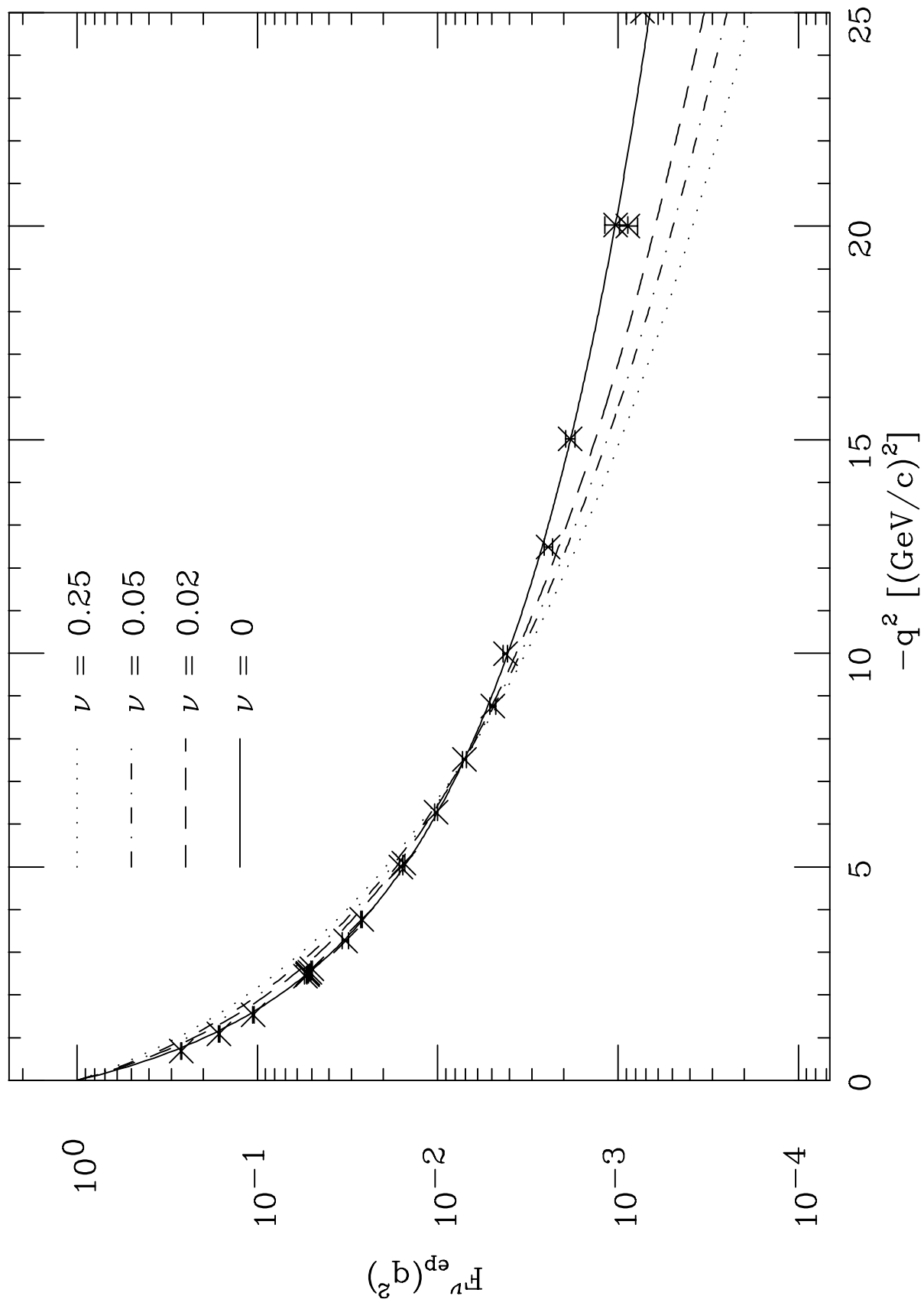


Fig.2

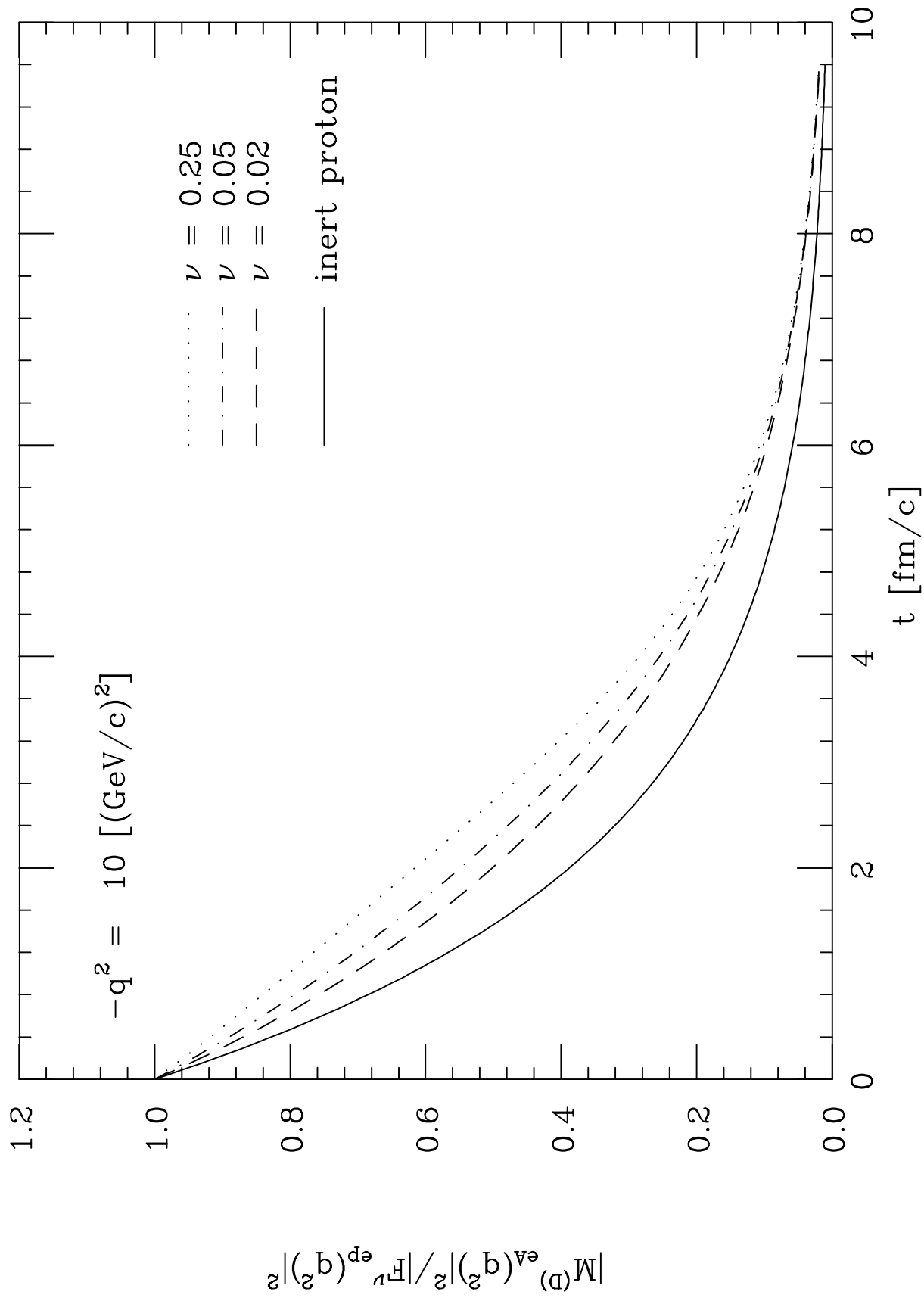


Fig.3

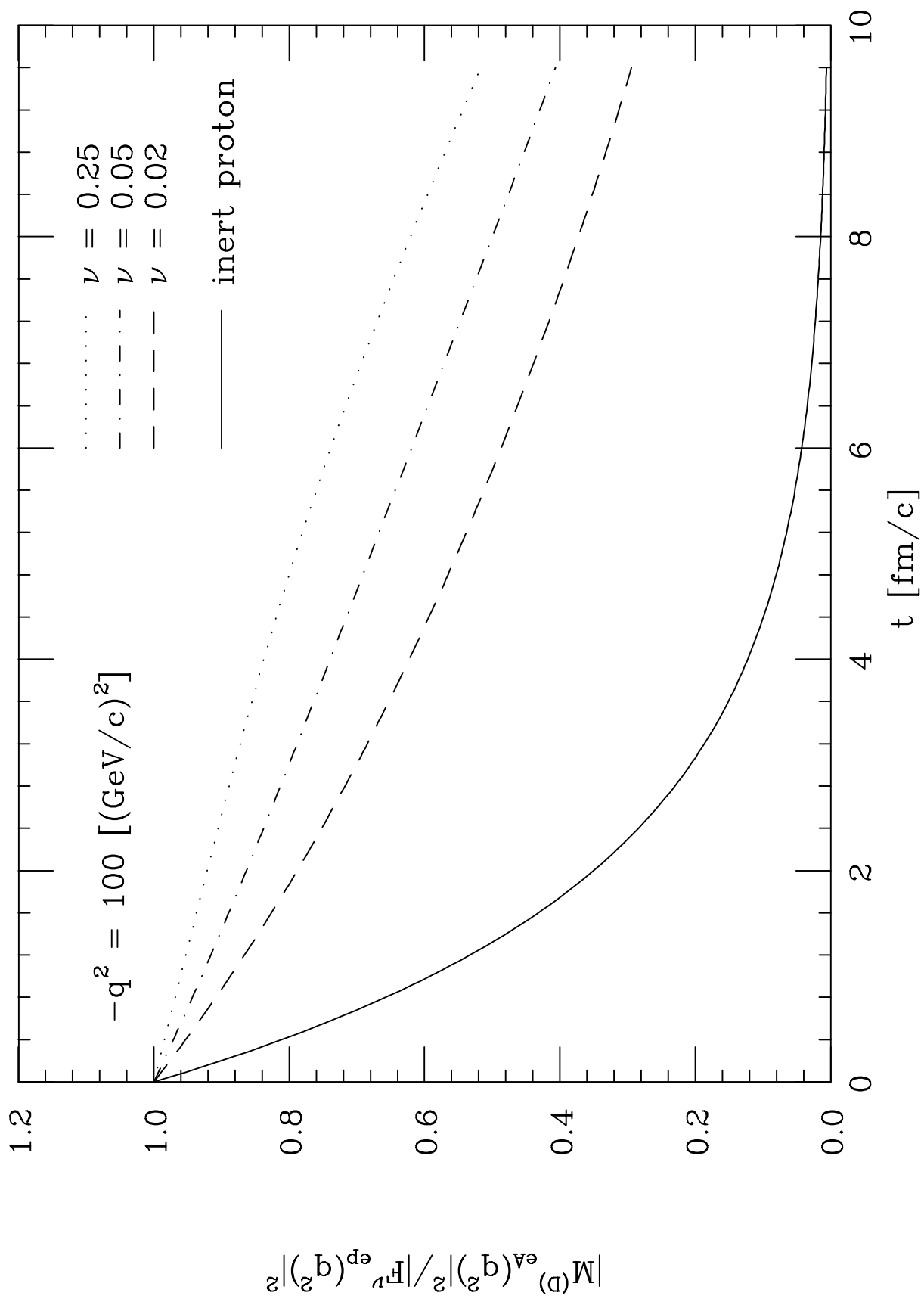


Fig. 4

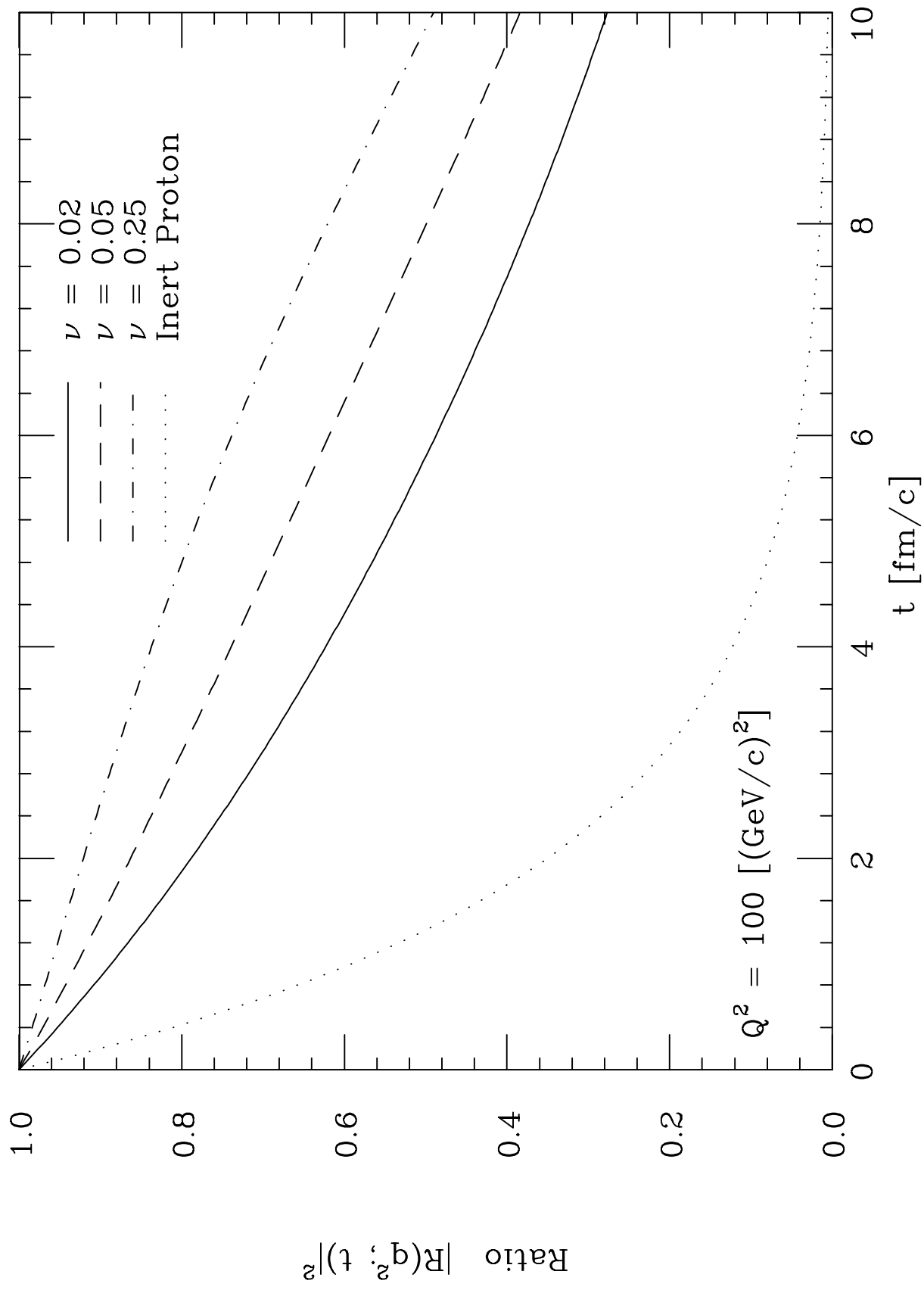


Fig. 5

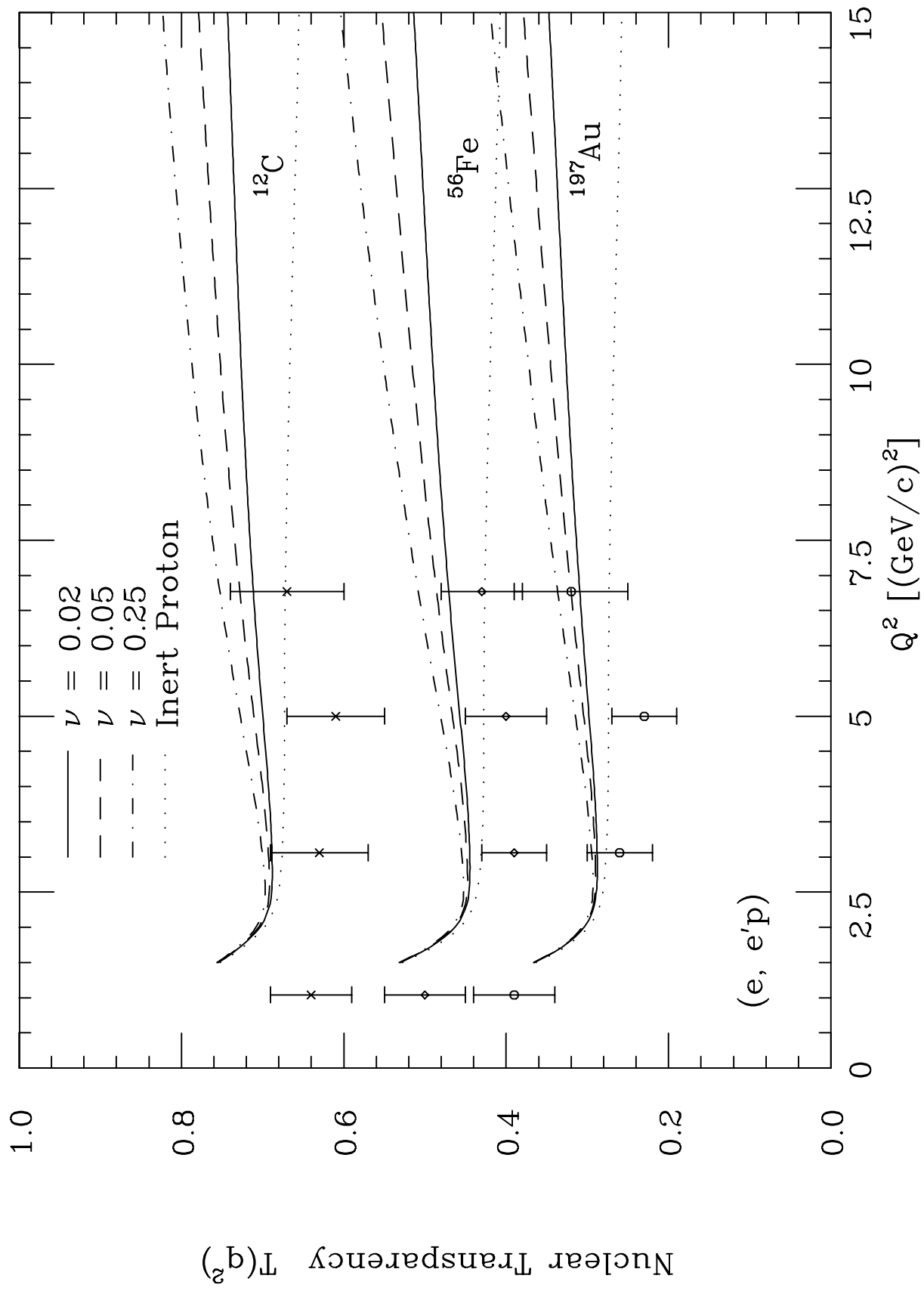


Fig. 6

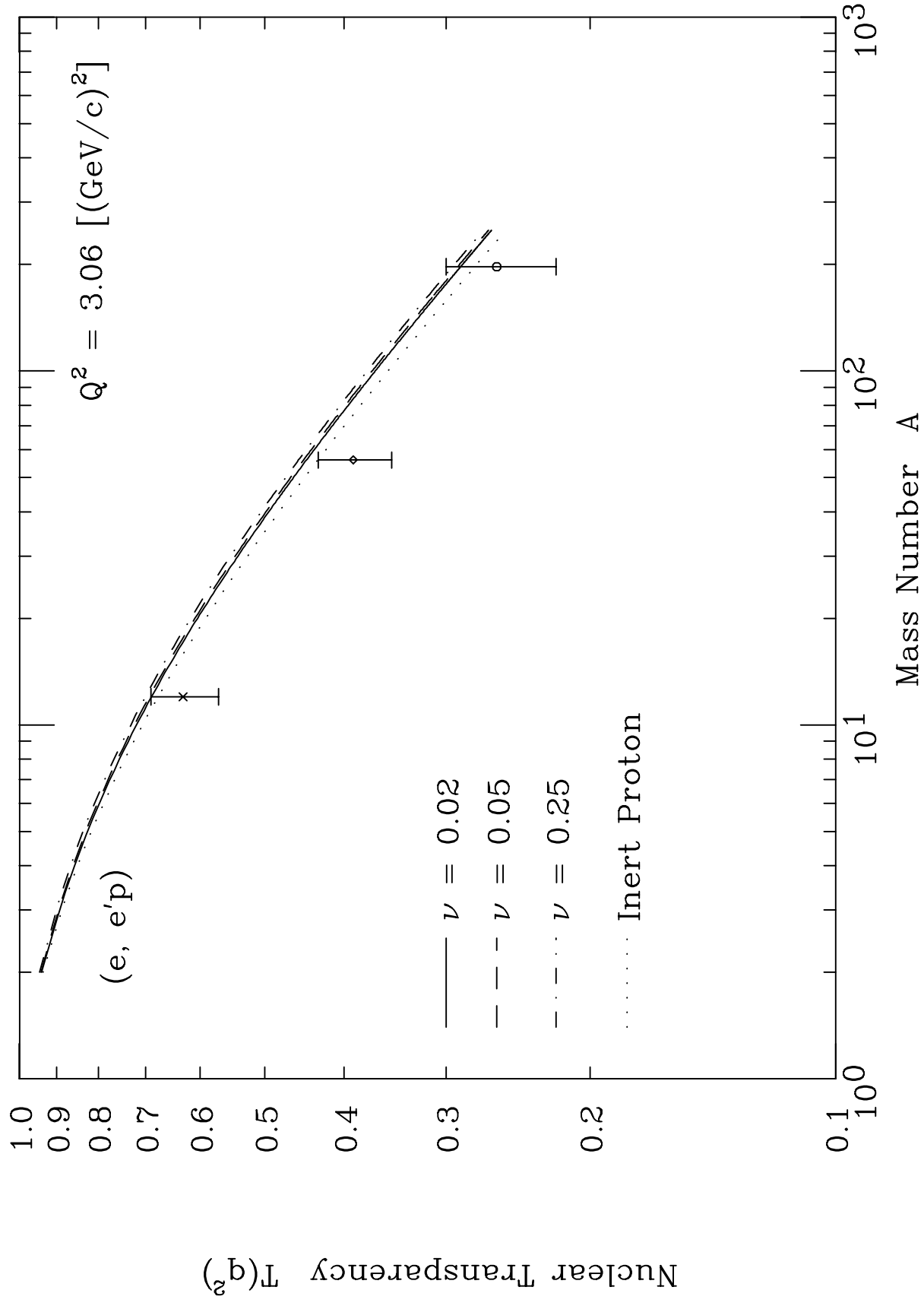


Fig. 7

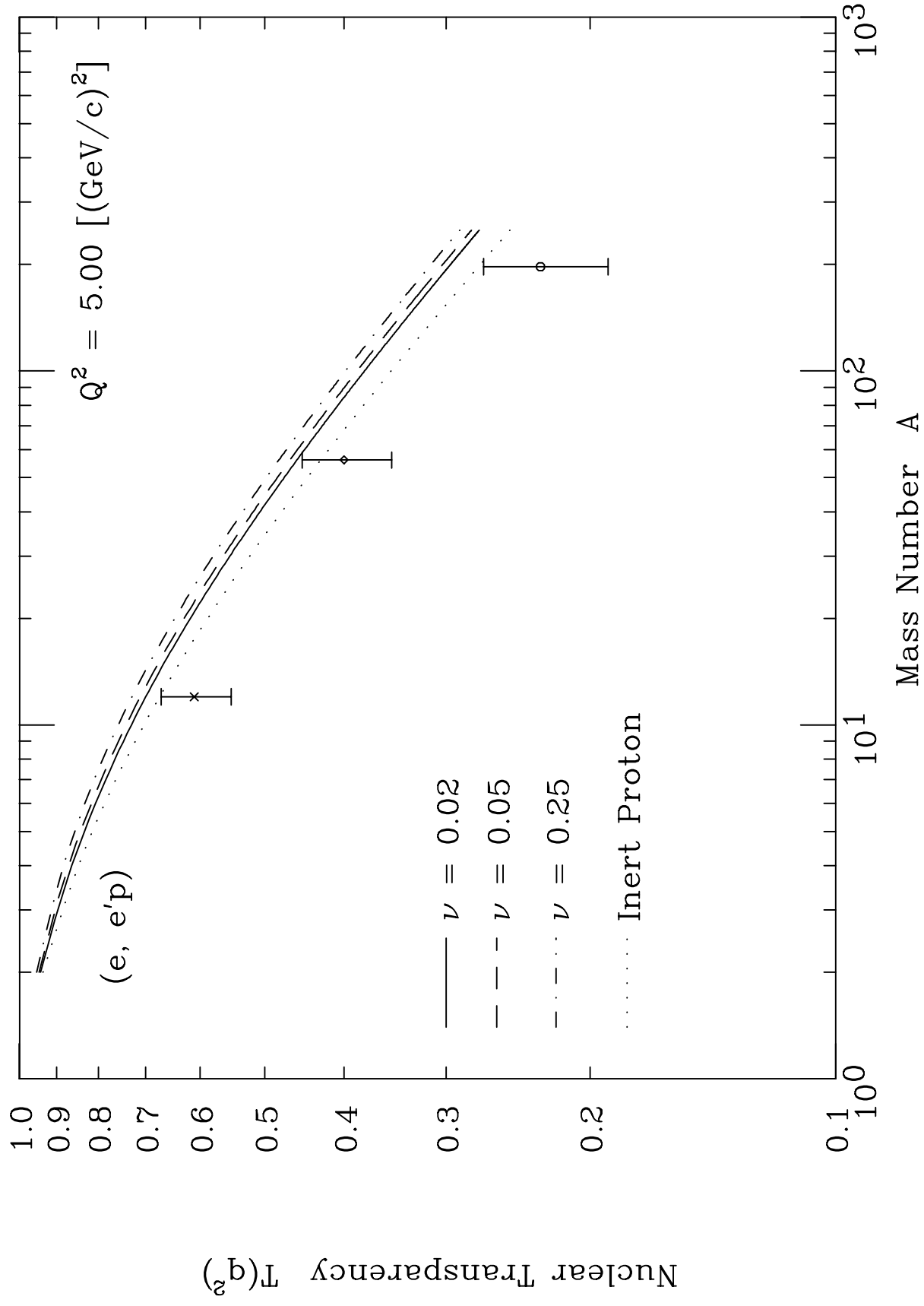


Fig. 8

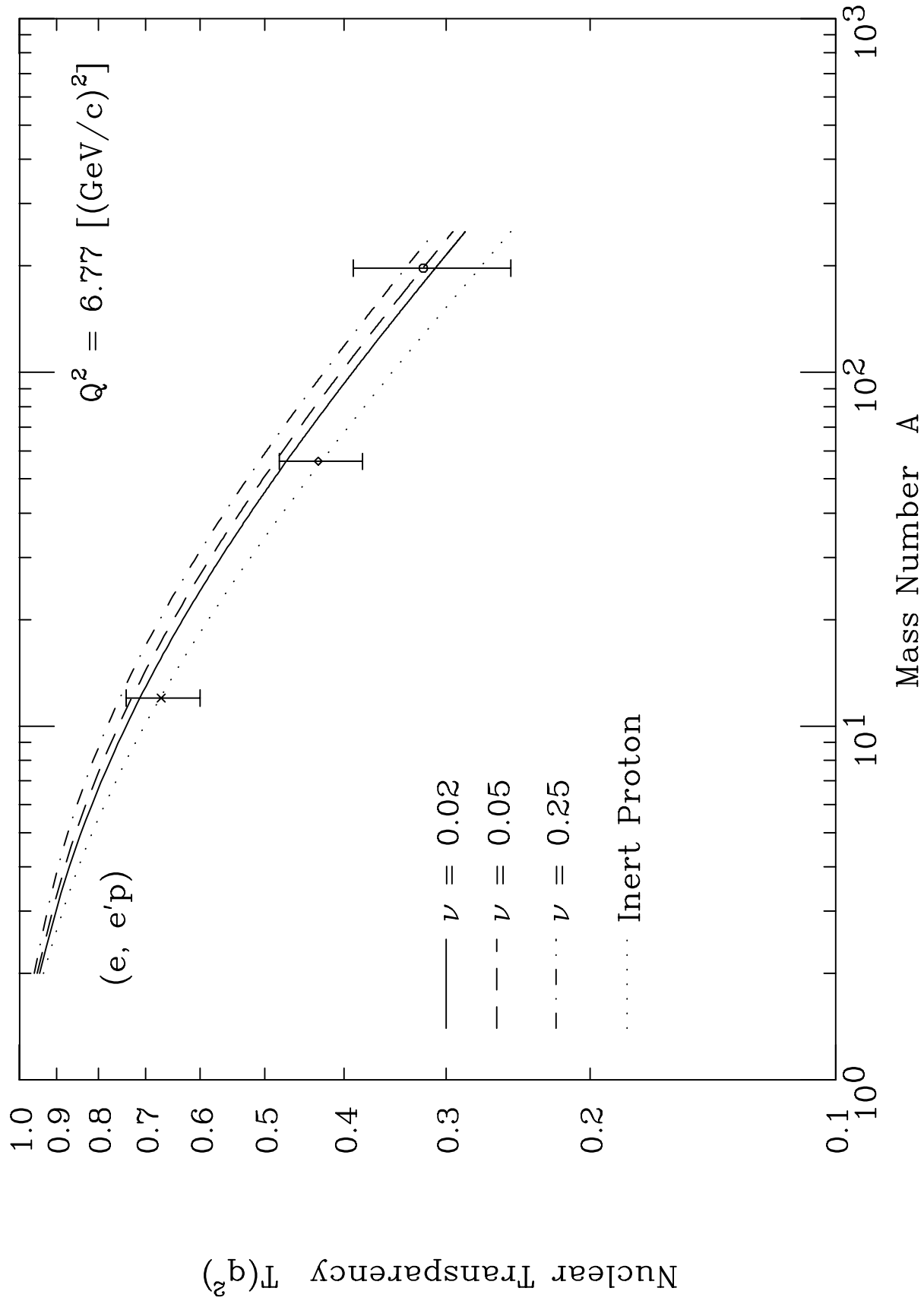


Fig. 9

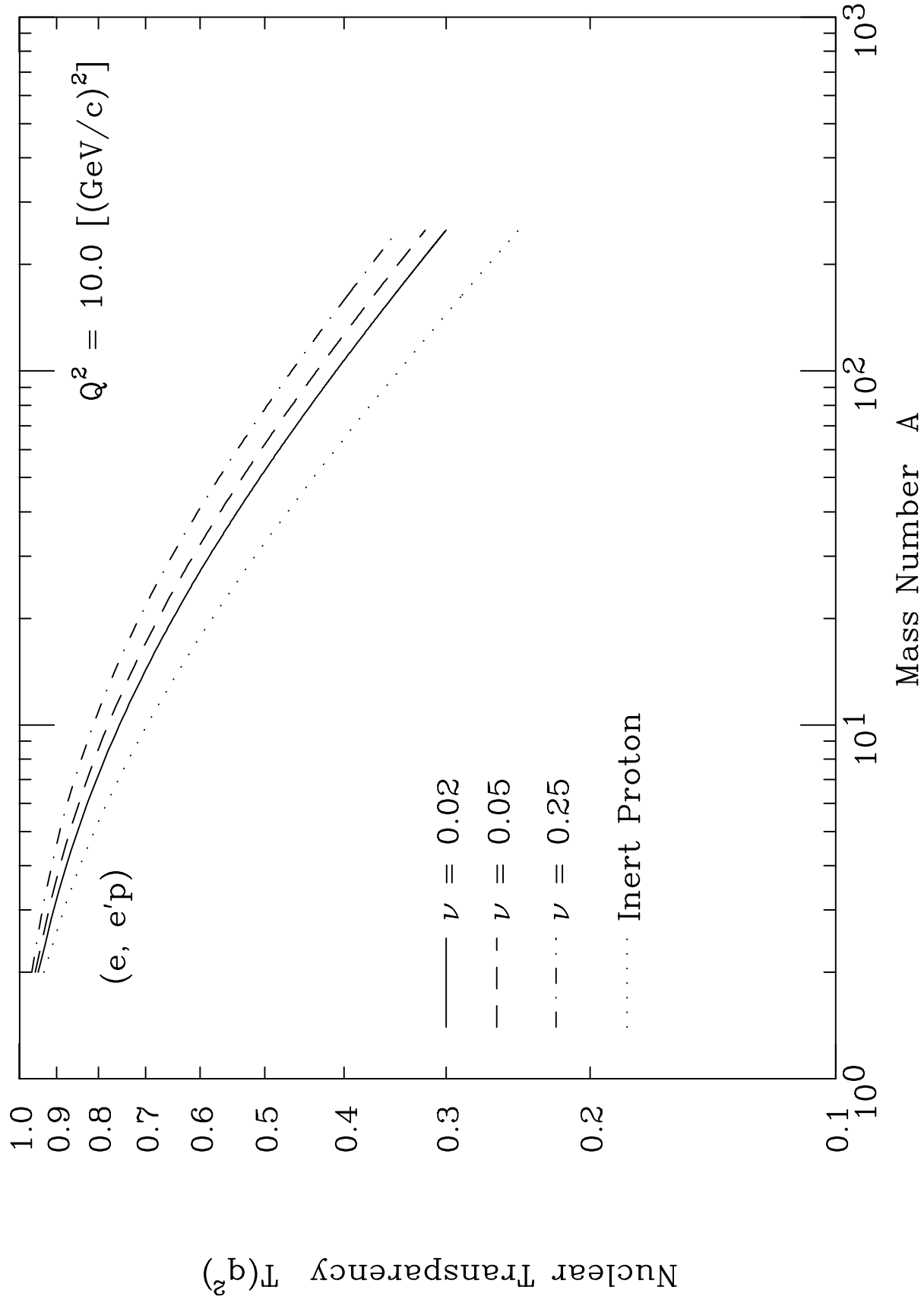


Fig. 10

